Inorg. Chem. **2008**, *47*, 8069−8076

Vapochromic Behavior of $\{Ag_2(Et_2O)_2[Au(C_6F_5)_2]_2\}_n$ with Volatile Organic Compounds

Eduardo J. Fernández, José M. López-de-Luzuriaga,* Miguel Monge, M. Elena Olmos, Raquel C. Puelles, Antonio Laguna, Ahmed A. Mohamed, and John P. Fackler, Jr.*

Departamento de Química, Universidad de La Rioja, Grupo de Síntesis Química de La Rioja, UA-CSIC, Madre de Dios 51, E-26004 Logroño, Spain, Departamento de Química Inorgánica-ICMA, Universidad de Zaragoza-CSIC, E-50009 Zaragoza, Spain, and Department of Chemistry and Laboratory for Molecular Structure and Bonding, Texas A&M University, P.O. Box 30012 College Station, Texas 77842-3012

Received March 11, 2008

The vapochromic behaviors of $\{Ag_2L_2[Au(C_6F_5)_2]_2\}_n$ (L = Et_2O (**1**), Me_2CO (**2**), THF (**3**), CH_3CN (**4**)) were studied. $\{Ag_2L_2[Au(C_6F_5)_2]_2\}_n$ (L = Et_2O (**1**)) was synthesized by the reaction of $[Bu_4N][Au(C_6F_5)_2]$ with $AgOClO_3$ in 1:1 molar ratio in CH_2Cl_2/Et_2O (1:2). **1** was used as starting material with THF to form $\{Ag_2L_2[Au(C_6F_5)_2]_2\}_n$ (L = THF (**3**)). **3** crystallizes in the monoclinic space group *C*2/*c* and consists of tetranuclear units linked together via aurophilic contacts resulting in the formation of a 1D polymer that runs parallel to the crystallographic *z* axis. The gold(I) atoms are linearly coordinated to two pentafluorophenyl groups and display additional Au···Ag close contacts within the tetranuclear units with distances of 2.7582(3) and 2.7709(3) Å. Each silver(I) center is bonded to the two oxygen atoms of the THF molecules with a Ag−O bond distance of 2.307(3) Å. TGA analysis showed that **1** loses two molecules of the coordinated solvent per molecular unit (1st one: 75−100°, second one: 150−175 °C), whereas **2**, **3**, and **4** lose both volatile organic compounds (VOCs) and fluorinated ligands in a less well defined manner. Each complex loses both the fluorinated ligands and the VOCs by a temperature of about 325 °C to give a 1:1 gold/silver product. X-ray powder diffraction studies confirm that the reaction of vapors of VOCs with **1** in the solid state produce complete substitution of the ether molecules by the new VOC. The VOCs are replaced in the order CH_3CN > Me_2CO > THF > Et_2O, with the ether being the easiest to replace. $\{Ag_2(Et_2O)_2[Au(C_6F_5)_2]_2\}_n$ and $\{Ag_2(THF)_2[Au(C_6F_5)_2]_2\}_n$ both luminesce at room temperature and at 77 K in the solid state. Emission maxima are independent of the excitation wavelength used below about 500 nm. Emission maxima are obtained at 585 nm (ether) and 544 nm (THF) at room temperature and at 605 nm (ether) and 567 nm (THF) at 77 K.

Introduction

The design and synthesis of stable and reversible chemical sensors have received increasing attention in the past few years. Vapochromic or vapoluminescent materials, which show dramatic color or luminescence change upon exposure to vapors of volatile organic compounds (VOCs), have been the focus of many studies due to their potential applications.[1–13] Different types of complexes, which include a variety of metal centers, such as Re/Co,[1] Ru,[2,3] Sn,[4] Pt,[5,6] Pt/M (M = Pd, Pt),[7] Cu,[8,9] Au[10,11] or Au/heterometal[12–14] have been reported. Among these are mononuclear[2–5] complexes, oligomeric species such as Balch's trinuclear $[Au_3(CH_3N{=}COCH_3)_3]$,[10b,c] polymeric materials formed via

* To whom correspondence should be addresed. E-mail: fackler@mail.chem.tamu.edu.

(1) Beauvais, L. G.; Shores, M. P.; Long, J. R. *J. Am. Chem. Soc.* **2000**, *122*, 2763.

(2) (a) Chang, Q.; Murtaza, Z.; Lakowicz, J. R.; Rao, G. *Anal. Chim. Acta* **1997**, *350*, 97. (b) Murphy, C. J.; Drane, W. D. *Proc. SPIE - Int. Soc. Opt. Eng.* **1995**, *2388*, 266. (c) Bignozzi, C. A.; Chiorboli, C.; Indelli, M. T.; Rampi, M. A.; Varani, G.; Scandola, F. *J. Am. Chem. Soc.* **1986**, *108*, 7872. (d) Winkler, J. R.; Creutz, C.; Sutin, N. *J. Am. Chem. Soc.* **1987**, *109*, 3470. (e) Scandolla, F.; Indelli, M. T. *Pure Appl. Chem.* **1988**, *60*, 973. (f) Kato, M.; Yamauchi, S.; Hirota, N. *J. Phys. Chem.* **1989**, *93*, 3422. (g) Posse, M. E. G.; Katz, N. E.; Baraldo, L. M.; Polonuer, D. D.; Colombano, C. G.; Olabe, J. A. *Inorg. Chem.* **1995**, *34*, 1830. (h) Waldhör, E.; Poppe, J.; Kaim, W. *Inorg. Chem.* **1995**, *34*, 3093. (i) Samuels, A. C.; DeArmond, M. K. *Inorg. Chem.* **1995**, *34*, 5548. (j) Timpson, C. J.; Bignozzi, C. A.; Sullivan, B. P.; Kober, E. M.; Meyer, T. J. *J. Phys. Chem.* **1996**, *100*, 2915. (k) Rampi, M. A.; Indelli, M. T.; Scandola, F.; pina, F.; Parola, A. J. *Inorg. Chem.* **1996**, *35*, 3355.

10.1021/ic800452w CCC: $40.75 © 2008 American Chemical Society
Published on Web 08/09/2008

metal−metal interaction such as stacked square-planar complexes of platinum and/or palladium salts reported by Mann and co-workers,[7] the Au/Tl linear polymer $[TlAu(C_6Cl_5)_2]_n$ with Au···Tl interactions,[12] and coordination polymers such as $\{Cu[Au(CN)_2]_2(DMSO)_2\}_n$.[13] All of these compounds show significant changes in their optical properties in the presence of solvents[1,2,8,10] or vapors of different VOCs.[3–7,9,11–14] These spectroscopic observations sometimes have been associated with the appearance of new bonding interactions such as weak hydrogen bonding,[5a,6] aurophilic contacts,[10a,11] solvent−metal bonds,[12] or reversible isomerization processes, as observed between $[CuI(4\text{-pic})]_\infty$ (pic = methylpicridine) and $[CuI(4\text{-pic})]_4$ when the former is exposed to liquid or vapor toluene.[9]

The incorporation of the organic vapor into the solid phase sometimes improves the packing in the crystal lattice by filling some of the free volume with the VOCs. A reversible solvent exchange can be favored when an anisotropic packing is present in the host material, as, for example, in the case of polymeric complexes,[7,12,13] in which the voids allow the vapor inclusion. This causes color change due to hydrogen bond formation, expansion, or contraction of the unit cell,[7] or covalent interaction of the VOC with a metal center such as thallium or copper.[13] The 1D network of $[TlAu(C_6Cl_5)_2]_n$ displays channels parallel to the *z* axis with diameters as large as 10.471 Å, which allow the VOCs to enter the lattice and interact with the Tl(I) centers to produce changes in the optical properties.[12]

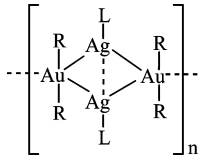

Although the synthesis of polymeric Au−Ag materials of the type $\{Ag_2L_2[Au(C_6F_5)_2]_2\}_n$ (L = neutral ligand, Sketch) by reaction of $[Au(C_6F_5)_2]^-$ with silver salts was reported by some of us more than 20 years ago,[15] it was only at the beginning of this century that their study was reinstated. The solid-state structures, which consist of tetranuclear Ag_2Au_2 units linked through unsupported Au···Au interactions, makes them very attractive from a photophysical point of view. This class of materials oligomerizes in solution, mediated by Au···Au interactions, upon increasing concentration.[16] They are promising VOC sensors because of the lability of ligands such as Et_2O in the coordination sphere of silver.[17]

This article details the properties of the extended linear chain Au^I/Ag^I complexes $\{Ag_2L_2[Au(C_6F_5)_2]_2\}_n$ (L = Et_2O, Me_2CO, THF, CH_3CN). Thermogravimetric analysis, powder and/or crystal X-ray diffraction, FTIR, UV−vis absorption, and luminescence measurements have been performed and the results are described here. The interconversion between these species is also studied and related to the donor ability of the oxygen- or nitrogen-donor molecules.

Instrumentation. Infrared spectra were recorded in the 4000−200 cm^{-1} range on a Nicolet Nexus FTIR using Nujol mulls between polyethylene sheets. Carbon, hydrogen, nitrogen, and sulfur analyses were carried out with a Perkin-Elmer 240C microanalyzer. Mass spectra were recorded on a Microflex MALDI-TOF Bruker spectrometer operating in the linear and reflector modes using dithranol as a matrix. ^1H and ^{19}F NMR spectra were recorded on a Bruker ARX 300 in $CDCl_3$ solutions. Chemical shifts are quoted relative to $SiMe_4$ (^1H, external) and $CFCl_3$ (^{19}F, external). Absorption spectra in solution were recorded on a Hewlett-Packard 8453 diode array UV−vis spectrophotometer. Excitation and emission spectra were recorded on a Jobin-Yvon Horiba Fluorolog 3−22 Tau-3 spectrofluorimeter. Fluorescence lifetime measurements were recorded while operating in the phase-modulation mode. The phase shift and modulation were recorded over the frequency range 0.1−10 MHz and data were fitted using the *Jobin-Yvon* software package. Thermogravimetric analyses (TGA) were recorded on a TA Instrument SDT 2960 using 2−10 mg samples at a 10 °C/min rate in 40−600 °C range under nitrogen, and in the 600−750 °C range in air.

Crystallography. A crystal of **3** was mounted in mineral oil on a glass fiber and transferred to the cold stream of a Nonius Kappa CCD diffractometer equipped with an Oxford Instruments low-temperature attachment. Data were collected

(3) Evju, J. K.; Mann, K. R. *Chem. Mater.* **1999**, *11*, 1425.
(4) Baldauff, E. A.; Buriak, J. M. *Chem. Commun.* **2004**, 2028.
(5) (a) Lu, W.; Chan, M. C. W.; Zhu, N.; Che, C. M.; He, Z.; Wong, K. Y. *Chem.−Eur. J.* **2003**, *9*, 6155. (b) Drew, S. M.; Janzen, D. E.; Buss, C. E.; MacEwan, D. I.; Dublin, K. M.; Mann, K. R. *J. Am. Chem. Soc.* **2001**, *123*, 8414.
(6) Buss, C. E.; Mann, K. R. *J. Am. Chem. Soc.* **2002**, *124*, 1031.
(7) (a) Grate, J. W.; Moore, L. K.; Janzen, D. E.; Veltkamp, D. J.; Kaganove, S.; Drew, S. M.; Mann, K. R. *Chem. Mater.* **2002**, *14*, 1058. (b) Exstrom, C. L.; Sowa, J. R., Jr.; Daws, C. A.; Janzen, D.; Mann, K. R. *Chem. Mater.* **1995**, *7*, 15. (c) Daws, C. A.; Exstrom, C. L.; Sowa, J. R., Jr.; Mann, K. R. *Chem. Mater.* **1997**, *9*, 363. (d) Buss, C. E.; Anderson, C. E.; Pomije, M. K.; Lutz, C. M.; Britton, D.; Mann, K. R. *J. Am. Chem. Soc.* **1998**, *120*, 7783. (e) Exstrom, C. L.; Pomije, M. K.; Mann, K. R. *Chem. Mater.* **1998**, *10*, 942.
(8) Dias, H. V. R.; Diyabalanage, H. V. K.; Rawashdeh-Omary, M. A.; Franzman, M. A.; Omary, M. A. *J. Am. Chem. Soc.* **2003**, *125*, 12072.
(9) Cariati, E.; Bu, X.; Ford, P. C. *Chem. Mater.* **2000**, *12*, 3385.
(10) (a) White-Morris, R. L.; Olmstead, M. M.; Jiang, F.; Tinti, D. S.; Balch, A. L. *J. Am. Chem. Soc.* **2002**, *124*, 2327. (b) Vickery, J. C.; Olmstead, M. M.; Fung, E. Y.; Balch, A. L. *Angew. Chem., Int. Ed. Engl.* **1997**, *36*, 1179. (c) Fung, E. Y.; Olmstead, M. M.; Vickery, J. C.; Balch, A. L. *Coord. Chem. Rev.* **1998**, *171*, 151.
(11) Mansour, M. A.; Connick, W. B.; Lachicotte, R. J.; Gysling, H. J.; Eisenberg, R. *J. Am. Chem. Soc.* **1988**, *120*, 1329.
(12) (a) Fernández, E. J.; López-de-Luzuriaga, J. M.; Monge, M.; Olmos, M. E.; Pérez, J.; Laguna, A.; Mohamed, A. A.; Fackler, J. P. *J. Am. Chem. Soc.* **2003**, *125*, 2022. (b) Fernández, E. J.; López-de-Luzuriaga, J. M.; Monge, M.; Montiel, M.; Olmos, M. E.; Pérez, J.; Laguna, A.; Mendizábal, F.; Mohamed, A. A.; Fackler, J. P. *Inorg. Chem.* **2004**, *43*, 3573.
(13) Lefebvre, J.; Batchelor, R. J.; Leznoff, D. B. *J. Am. Chem. Soc.* **2004**, *126*, 16117.
(14) (a) Bariain, C.; Matías, I. R.; Fdez-Valdivielso, C.; Elosúa, C.; Luquín, A.; Garrido, J.; Laguna, M. *Sens. Actuators, B* **2005**, *108*, 535. (b) Luquín, A.; Bariain, C.; Vergara, E.; Cerrada, E.; Garrido, J.; Matias, I. R.; Laguna, M. *Appl. Organomet. Chem.* **2005**, *19*, 1232.
(15) (a) Usón, R.; Laguna, A.; Laguna, M.; Jones, P. G.; Sheldrick, G. M. *Chem. Commun.* **1981**, 1097. (b) Usón, R.; Laguna, A.; Laguna, M.; Manzano, B. R.; Jones, P. G.; Sheldrick, G. M. *J. Chem. Soc., Dalton Trans.* **1984**, 285.
(16) Fernández, E. J.; Gimeno, M. C.; Laguna, A.; López-de-Luzuriaga, J. M.; Monge, M.; Pyykkö, P.; Sundholm, D. *J. Am. Chem. Soc.* **2000**, *122*, 7287.
(17) Fernández, E. J.; Laguna, A.; López-de-Luzuriaga, J. M.; Monge, M. *Spanish Patent P200001391*, 2003.

Table 1. Data Collection and Structure Refinement Details for **3**

compound	**3**
chemical formula	$C_{32}H_{16}Ag_2Au_2F_{20}O_2$
cryst habit	green block
cryst size/mm	0.18 × 0.15 × 0.12
cryst syst	monoclinic
space group	*C*2/*c*
a/Å	18.2661(9)
b/Å	13.4827(6)
c/Å	15.0525(8)
β/°	109.204(2)
U/Å^3	3500.8(3)
Z	4
D_{calcd}/g cm^{-3}	2.698
M	1422.12
F(000)	2624
T/°C	−100
$2\theta_{max}$/°	56
μ(Mo Kα)/mm^{-1}	9.597
no. of reflns measured	15 423
no. of unique reflns	4069
R_{int}	0.0381
R[a] ($I > 2\sigma(I)$)	0.0245
wR[b] (F^2, all reflns)	0.0501
no. of params	271
no. of restraints	40
S[c]	1.073
max. Δρ/e Å^{-3}	2.083

[a] $R(F) = \Sigma||F_o| - |F_c||/\Sigma|F_o|$. [b] $wR(F^2) = [\Sigma\{w(F_o^2 - F_c^2)^2\}/\Sigma\{w(F_o^2)^2\}]^{0.5}$; $w^{-1} = \sigma^2(F_o^2) + (aP)^2 + bP$, where $P = [F_o^2 + 2F_c^2]/3$ and *a* and *b* are constants adjusted by the program. [c] $S = [\Sigma\{w(F_o^2 - F_c^2)^2\}/(n - p)]^{0.5}$, where *n* is the number of data and *p* the number of parameters.

Table 2. Selected Bond Lengths [Angstroms] and Angles [Degrees] for **3**[a]

Au−C(1)#1	2.065(4)
Au−C(11)	2.067(4)
Ag−O	2.307(3)
Ag−C(11)	2.468(4)
Ag−C(1)	2.492(4)
Ag−Au#1	2.7582(3)
Ag−Au	2.7709(3)
Ag−Ag#1	3.2291(6)
Au−Au#2	3.1959(3)
C(1)#1−Au−C(11)	175.09(16)
C(11)−Ag−C(1)	131.87(14)

[a] Symmetry transformations used to generate equivalent atoms: #1, $-x$, $-y + 2$, $-z$; #2, $-x$, y, $-z + {}^1/_2$.

by monochromated Mo Kα radiation ($\lambda = 0.71073$ Å) with scan types ω and ϕ and numerical absorption correction (based on multiple scans). The structure was solved by direct methods and refined on F^2 using *SHELXL-97*.[18] All non-hydrogen atoms were anisotropically refined and hydrogen atoms were included using a riding model. One of the carbon atoms of the THF molecule is disordered over two different positions (60:40). Further details regarding the data collection and refinement methods are listed in Table 1. Selected bond lengths and angles are listed in Tables 1 and 2 and the crystal structure of **3** is shown in Figures 1 and 2. X-ray powder diffraction patterns were obtained at room temperature using a Bruker-AXS D8 Advanced Bragg−Brentano X-ray Powder diffractometer equipped with a single-crystal graphite monochromator and a scintillation counter or a Rigaku RU300 rotating anode generator by using graphite-monochromated CuK operating at 40 kV and 80 mA. Powder diffraction patterns were collected between 2θ of 5° and 60° with a 2θ stepping angle of 0.03° and an angle dwell of 1 s.

(18) Sheldrick, G. M. *SHELXL-97, Program for Crystal Structure Refinement*; University of Göttingen: Göttingen, Germany, 1997.

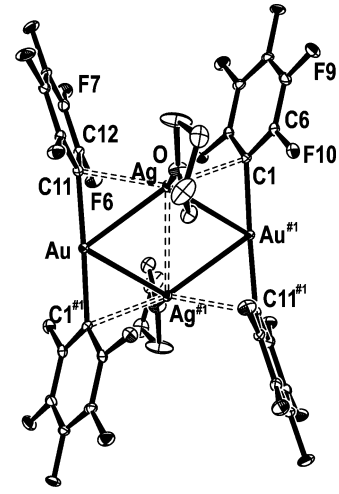

Figure 1. Tetranuclear unit of **3** with the labeling scheme for the atom positions. Hydrogen atoms have been omitted for clarity.

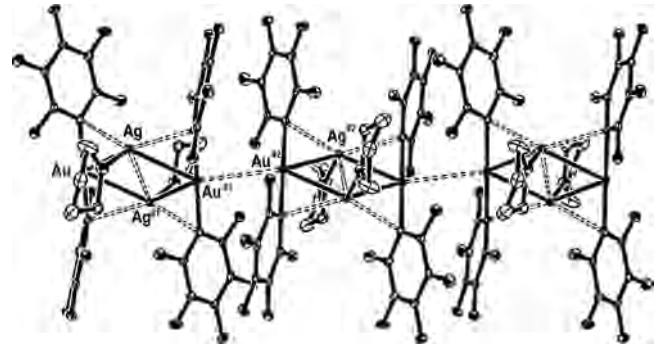

Figure 2. A portion of the polymeric structure of **3**. Hydrogen atoms have been omitted for clarity.

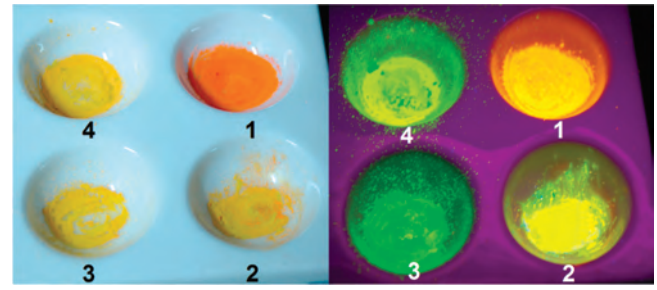

Figure 3. Left: Powder samples of $\{[AuAg(C_6F_5)_2(Et_2O)]_2\}_n$ (**1**) exposed to selected organic vapors: acetone (**2**), THF (**3**), and acetonitrile (**4**). Right: The same samples on the left but under UV light (365 nm).

General Comments. All the volatile organic compounds were purchased from Panreac. The complexes $[Bu_4N][Au(C_6F_5)_2]$ and $\{Ag_2L_2[Au(C_6F_5)_2]_2\}_n$ (L = Me_2CO, **2**; CH_3CN, **4**)[16,19] were synthesized according to literature procedures. Solvents used in the spectroscopic studies were degassed prior to use. Exchange reactions of the solids with VOCs were carried out at room temperature by passing a stream of nitrogen gas over the liquid VOC and running the VOC saturated nitrogen over the sample. Color changes took place in a few seconds. ***Caution!*** *Perchlorate salts may be explosive or cause explosions to occur in the presence of organics.*

(19) Fernández, E. J.; Laguna, A.; López-de-Luzuriaga, J. M.; Monge, M.; Montiel, M.; Olmos, M. E.; Rodríguez-Castillo, M. *Organometallics* **2006**, *25*, 3639.

Synthesis of $\{Ag_2L_2[Au(C_6F_5)_2]_2\}_n$ (L = Et_2O, 1). To a CH_2Cl_2/Et_2O solution (1:2) of $[Bu_4N][Au(C_6F_5)_2]$ (0.116 g, 0.150 mmol) was added $AgOClO_3$ (0.031 g, 0.150 mmol). A deep-orange solid formed immediately and was filtered after 30 min stirring.(Yield: 91%). ^{1}H NMR (300.13 MHz, 298 K, $CDCl_3$, ppm): 3.46 (s, 2H, $^2J(H-H) = 7$ Hz, CH_2) and 1.21 (t, 3H, $^2J(H-H) = 7$ Hz Me); ^{19}F NMR (282.4 MHz, 298 K, $CDCl_3$, ppm): −110.17 (m, 4F, F_o), −150.74 (m, 2F, F_p), −160.50 (m, 4F, F_m); MALDI-TOF (-): *m/z* 531 $[Au(C_6F_5)_2]^-$ 100%, 865 $[Au(C_6F_5)_4]^-$ 20%, 1169 $[Au_2Ag(C_6F_5)_4]^-$ 27%; MALDI-TOF (+) *m/z:* 333 [dithranol + Ag]$^+$ 57%; FTIR (*Nujol mull*) ν (Au−C_6F_5) at 1505, 964, 786 cm^{-1}; elemental Anal. Calcd (%) for $C_{32}H_{20}Ag_2Au_2F_{20}O_2$: C 26.97, H 1.42; found: C 26.83, H 1.63.

Synthesis of $\{Ag_2L_2[Au(C_6F_5)_2]_2\}_n$ (L = THF, 3). A solution of **1** (0.088 g, 0.4 mmol) in THF (10 mL) was stirred for 10 min. Evaporation of the solvent to dryness gave a green solid in an almost quantitative yield. ^{1}H NMR (300.13 MHz, 298 K, $CDCl_3$, ppm): 3.73 (m, 2H, CH_2O) and 1.84 (m, 2H, CH_2); ^{19} F NMR (282.4 MHz, 298 K, $CDCl_3$, ppm): −110.64 (m, 4F, F_o), −150.62 (m, 2F, F_p), −160.18 (m, 4F, F_m); MALDI-TOF (-): *m/z* 531 $[Au(C_6F_5)_2]^-$ 100%, 865 $[Au(C_6F_5)_4]^-$ 35%, 1169 $[Au_2Ag(C_6F_5)_4]^-$ 13%; MALDI-TOF (+) *m/z:* 333 [dithranol + Ag]$^+$ 50%; FT-IR (Nujol) ν (Au−C_6F_5) at 1505, 969, 783 cm^{-1} and ν (C−O−C) at 917 cm^{-1}; elemental Anal. Calcd (%) for $C_{32}H_{16}Ag_2Au_2F_{20}O_2$: C 27.04, H 1.13; found: C 27.11, H 1.23.

CCDC-679486 contains the supplementary crystallographic data for this paper. These data can be obtained free of charge via www.ccdc.cam.ac.uk/conts/retrieving.html (or from the Cambridge Crystallographic Data Centre, 12 Union Road, Cambridge CB2 1EZ, UK; fax: (+44) 1223−336−033; or e-mail: deposit@ccdc.cam.ac.uk).

Results and discussion

Synthesis and Characterization. The polymeric complex $\{Ag_2(Et_2O)_2[Au(C_6F_5)_2]_2\}_n$ **1**, was obtained by the reaction of $[Bu_4N][Au(C_6F_5)_2]$ with $AgClO_4$ in 1:1 molar ratio in CH_2Cl_2/Et_2O (1:2). **1** was used as a starting material for the synthesis of complexes $\{Ag_2L_2[Au(C_6F_5)_2]_2\}_n$ (L = Me_2CO, **2**; THF, **3**; CH_3CN, **4**). The synthesis of **2** and **4** have been previously reported by some of us.[16,19] All complexes showed the same stoichiometry and their structures consist of tetranuclear units connected through unsupported Au(I)···Au(I) contacts resulting in the formation of 1D polymer with different organic ligands bonded to Ag(I) centers. All compounds show characteristic and bright colors depending on the solvents, namely, orange for diethylether (**1**), yellow for acetone and acetonitrile (**2** and **4**), and green for THF (**3**). The solutions of these complexes are stable to air and moisture for hours without apparent decomposition in the dark. The presence of the organic ligands in **1** and **3** is also confirmed in their ^{1}H NMR spectra, which display two signals at 3.46 and 1.21 ppm and two multiplets at 3.73 and 1.84 ppm, corresponding to Et_2O and THF, respectively. The chemical shifts are similar to those of the free organic ligands in agreement with a dissociation process in solution. ^{19}F NMR spectra show the typical pattern of pentafluorophenyl groups bonded to gold(I) centers. The MALDI-TOF (matrix-assisted laser desorption/ionization-time-of-flight) for **1** and **3** display peaks at *m/z* = 333 (57% (**1**), 50% (**3**) [dithranol + Ag$^+$]), 531 (100% (**1** and **3**) $[Au(C_6F_5)_2]^-$) and 1169 (27% (**1**), 13% (**3**) $[Au_2Ag(C_6F_5)_4]^-$). The IR spectra for **1** and **3** in Nujol mulls show the $C_6F_5^-$ absorptions at 1505 cm^{-1}, 965−969 cm^{-1}, and 783−786 cm^{-1}, corresponding to the ν (C−F) and ν (Au−C) modes, respectively. Furthermore, **3** displays a band at 917 cm^{-1} that can be attributed to the THF (C−O−C) bend.

Crystal Structure of $\{Ag_2(THF)_2[Au(C_6F_5)_2]_2\}_n$. The crystals of **3** were obtained by slow diffusion of THF into a solution of the complex in CH_2Cl_2. It crystallizes in the monoclinic space group *C*2/*c* and consists of tetranuclear $\{Ag_2(THF)_2[Au(C_6F_5)_2]_2\}_n$ units (Figure 1) linked together via aurophilic contacts resulting in the formation of 1D polymer that runs parallel to the crystallographic *z* axis. The molecule lies on a 2-fold symmetry axis, so only half of the molecule resides in the asymmetric unit. The intermolecular Au−Au distance of 3.1959(3) Å is slightly longer than that found in the related complex $\{Ag_2(Me_2CO)_2[Au(C_6F_5)_2]_2\}_n$[16] (3.1674(11) Å) and appreciably longer than those observed in $\{Ag_2(C_6H_6)_2[Au(C_6F_5)_2]_2\}_n$[15b] (3.013(2) Å), $\{Ag_2(SC_4H_8)_2[Au(C_6F_5)_2]_2\}_n$[15a] (2.889(2) Å), or $\{M_2(NCCH_3)_2[Au(C_6F_5)_2]_2\}_n$ (M = Ag (2.8807(4) Å), Cu (2.9129(3) Å).[19]

The gold(I) atoms are linearly coordinated to two pentafluorophenyl groups and display additional Au−Ag contacts within the tetranuclear unit of 2.7582(3) and 2.7709(3) Å. These distances lie within the range 2.7267(5)−2.7903(9) Å for the Au−Ag contacts observed in the related complexes $\{Ag_2L_2[Au(C_6F_5)_2]_2\}_n$ (L = Me_2CO,[16] C_6H_6,[15b] SC_4H_8,[15a] or CH_3CN[19]). Each silver(I) center is also bonded to the oxygen atom of a THF molecule with a Ag−O bond distance of 2.307(3) Å, which is shorter than in the acetone complex $\{Ag_2(Me_2CO)_2[Au(C_6F_5)_2]_2\}_n$ (2.537(7) Å).[16] As in the acetonitrile and acetone derivatives, there is an additional Ag···Ag contact within the Ag_2Au_2 core of 3.2291(6) Å, although it is longer in **3** than in the acetonitrile (3.1084(10) Å)[19] or acetone (3.1810(13) Å)[16] complexes, which display very similar crystal structures. Another similarity between these structures is the presence of pentafluorophenyl groups acting as asymmetrical bridges between the gold and silver atoms (Figure 2) with Au−C distances of 2.065(4) and 2.067(4) Å and Ag−C distances of 2.468(4) and 2.492(4) Å.

Vapochromic Studies. As described above, exposure of $\{Ag_2(Et_2O)_2[Au(C_6F_5)_2]_2\}_n$, **1,** in the solid state at room temperature to vapors of the volatile organic compounds, employed as ligands for the synthesis of complexes **2**-**4**, leads to a quick, perceptible change in the color of the samples. The vapochromic behaviors of complexes **1**-**4** have been studied using thermogravimetric analysis (TGA), powder and/or single-crystal X-ray diffraction, FT-IR, UV−vis absorption, and luminescence measurements.

Thermogravimetric Studies. Thermogravimetric studies of the samples from the exposure of **1** to different organic vapors show that they lose different number of solvates per metallic cluster. At a temperature of about 325 °C, nearly

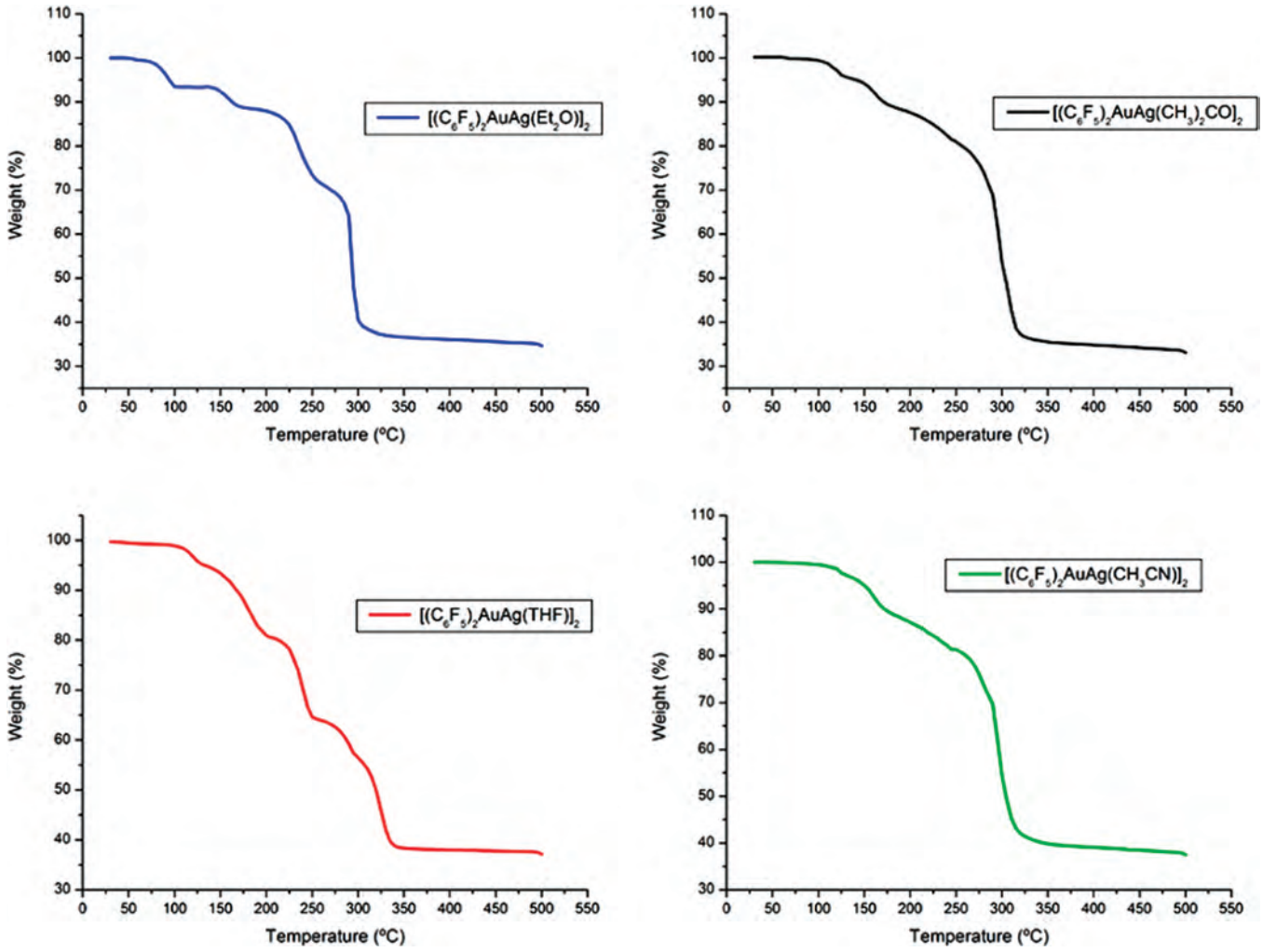

Figure 4. TGA traces for **1** (left, above) (blue), **2** (right, above) (black), **3** (left, below) (red), and **4** (right, below) (green).

all of the organic material is lost, leaving an equal amount of silver and gold. No additional data was obtained that relates to the nature of this product. Each of the four samples presented here show the same general pattern of weight loss. TGA trace for the ether complex **1** shows the clearest formation of intermediates. The first ether molecule appears to be lost between 75 and 100 °C, the second between 150−175 °C. From 220−300 °C, the fluorinated ligands are lost, probably as $C_6F_5-C_6F_5$. Indeed, this reductive elimination product was the only fluorinated product observed in the GC-MS of the ether derivative. With the acetone product, loss of this ligand appears between 110 and 160 °C but the steps are not clean and HC_6F_5 may also be lost along with $C_6F_5-C_6F_5$ to 325 °C. With the THF product, the first THF (about 5% of the weight) is lost between 100−125 °C, and from 125−225 °C it appears that both THF and HC_6F_5 or $C_6F_5-C_6F_5$ (or both fluorocarbons) are being lost. With the acetonitrile complex, both CH_3CN ligands appear to be lost between 115−150 °C but the plateaus are not clean and the fluorinated ligands also may be lost, which certainly happens between 150 and 325 °C. The observed variations in the temperature and percentage of VOC ligands lost are likely due to their different boiling points, the strengths of the interactions between the ligands with the silver centers, and the ease of VOC deprotonation (to form the volatile HC_6F_5) (Figure 4).

Powder Diffraction Studies of the Vapochromic Materials. X-ray powder diffraction (XPD) studies of the materials obtained upon exposure of the $\{Ag_2L_2[Au(C_6F_5)_2]_2\}_n$ (L = Et_2O, Me_2CO, THF, CH_3CN) complexes to different VOCs were carried out. The vapochromic behavior was analyzed first through the comparison of the XPD patterns before and after heating. Second, we studied the VOCs uptake ability for the $\{Ag_2(Et_2O)_2[Au(C_6F_5)_2]_2\}_n$ starting complex **1** by comparison of the XPD profiles with the profiles from the CIF files obtained from the X-ray analysis for complexes $\{Ag_2(Me_2CO)_2[Au(C_6F_5)_2]_2\}_n$ (**2**), $\{Ag_2(THF)_2[Au(C_6F_5)_2]_2\}_n$ (**3**), and $\{Ag_2(NCCH_3)_2[Au(C_6F_5)_2]_2\}_n$ (**4**). We have found that after heating the samples prepared by exposure of $\{Ag_2(Et_2O)_2[Au(C_6F_5)_2]_2\}_n$ to the VOCs, decomposition occurs and reversibility of the VOCs uptake delivery is not observed.

The starting material $\{Ag_2(Et_2O)_2[Au(C_6F_5)_2]_2\}_n$ (**1**) reacts with the ligands Me_2CO, THF, and CH_3CN[16,19] to form **2**−**4** characterized using X-ray diffraction analysis. The same **2**−**4** also can be obtained when Me_2CO, THF, and CH_3CN act as VOCs in the solid−gas reaction described above with **1**.

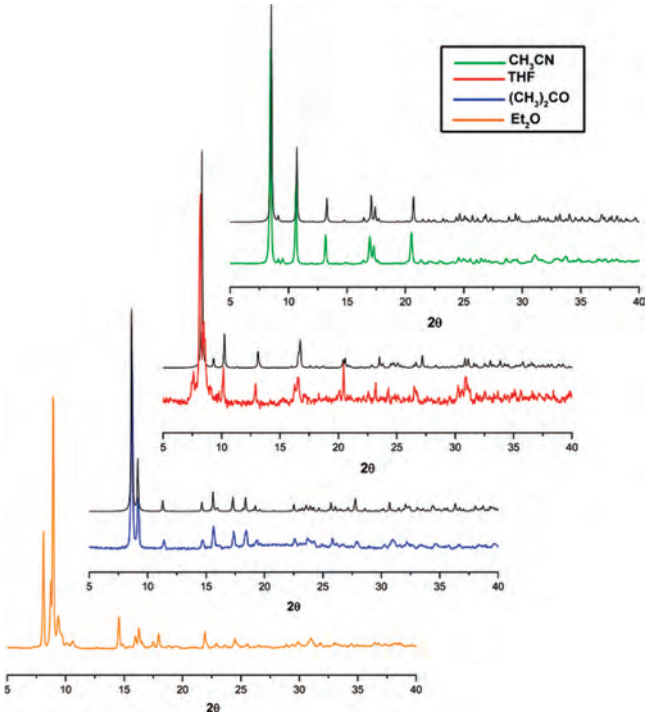

Figure 5. XPD diffraction patterns for VOC Au−Ag materials obtained by treatment of **1** (orange) with acetone (blue), THF (red), and acetonitrile (green) compared with the corresponding XPD pattern obtained from X-ray crystallography for **2**, **3**, and **4**, respectively (black).

The CIF files generated from X-ray crystallography match in all cases the XPD patterns obtained from the exposure of the powder samples to VOC vapors. This is in accord with a complete substitution of the very labile Et_2O ligand by the vapors of acetone, THF, and CH_3CN (Figure 5).

When $\{Ag_2(Me_2CO)_2[Au(C_6F_5)_2]_2\}_n$ (**2**) is treated with Et_2O or THF, the XPD patterns do not correspond either to the starting material **2** or to the possible final products **1** or **3**, and appears to be a mixture of compounds. When **2** is exposed to CH_3CN, the XPD pattern matches that for **4.** A complete substitution of ligands is achieved (Supporting Information).

$\{Ag_2(THF)_2[Au(C_6F_5)_2]_2\}_n$ (**3**) reacts partially with Et_2O leading to a mixture of **1** and **3** in the XPD spectrum. Interestingly, **3** reacts completely with Me_2CO and CH_3CN vapors, leading to **2** and **4**. When $\{Ag_2(NCCH_3)_2[Au(C_6F_5)_2]_2\}_n$ (**4**) was treated with the gaseous VOCs Et_2O, Me_2CO, and THF at room temperature, no reaction occurred, and, in all cases, the XPD profile for **4** was obtained. The XPD profiles for the reactions of $\{Ag_2(Me_2CO)_2[Au(C_6F_5)_2]_2\}_n$ (**2**) with CH_3CN and $\{Ag_2(NCCH_3)_2[Au(C_6F_5)_2]_2\}_n$ (**4**) with Me_2CO are shown in Figure 6.

Infrared Studies. Exposure of **1**, **2**, and **3** to CH_3CN vapor, as described above leads, in all cases, to IR spectra that clearly match the one from **4** with bands at 2315 and 2388 cm^{-1} that correspond to the $\nu(C\equiv N)$ vibration mode. These observations suggest a complete substitution of oxygen-donor ligands by the stronger nitrogen-donor ligands, CH_3CN, in agreement with the previously commented XPD results. The rest of the IR analyses are not conclusive because the characteristic bands associated with the VOCs are masked by other vibrations.

The studies presented (TGA, XPD) show the following conclusions. Whereas **1** easily loses (below 175 °C) 2 molecules of Et_2O per molecule of complex in the first step, the corresponding VOC materials with acetone and THF lose only one molecule easily (below 125°). With acetonitrile, the loss of both VOC and fluorinated ligands take place with no clear intermediate being formed. The donor ability of the VOCs to the silver centers impacts on its loss as does its volatility. Whereas the reductive elimination product $C_6F_5-C_6F_5$ has been observed in the mass spectrum of the ether product decomposition, HC_6F_5 also appears to account for the weight loss in some systems and especially with the VOC THF.

The XPD studies confirm that the absorption of organic VOCs by the solid complex **1** produces complete coordination of the silver center, unlike the partial coordination of thallium found in the thallium−gold complexes reported previously.[12] Moreover, the donor ability of the VOCs is easily classified (Scheme 1). The nitrogen-donor ligand CH_3CN is able to perform a complete substitution of the oxygen-donor ligands Et_2O, Me_2CO, and THF, but not vice versa. Among the oxygen-donor ligands, acetone shows the most complete donor ability because it can substitute fully both Et_2O and THF ligands but not vice versa. Finally, whereas THF is able to displace Et_2O from **1**, Et_2O is not able to displace THF in **3**. Therefore, the exchange ability of the VOCs with this silver complex follows the order $CH_3CN > Me_2CO > THF > Et_2O$, an order close to the order of the boiling points (vapor pressures) of the VOCs.

These studies demonstrate that the reactions between $\{Ag_2L_2[Au(C_6F_5)_2]_2\}_n$ *complexes and VOCs are substitution reactions rather than superficial adsorption processes*. We also observe that these exchange processes are not reversible, which suggests that similar behaviors described in the literature for related systems probably should be revisited.

Luminescence Studies. As was previously reported for $\{Ag_2(Me_2CO)_2[Au(C_6F_5)_2]_2\}_n$ (**2**)[16] and $\{Ag_2(NCCH_3)_2[Au(C_6F_5)_2]_2\}_n$ (**4**),[19] the compounds $\{Ag_2(Et_2O)_2[Au(C_6F_5)_2]_2\}_n$ (**1**) and $\{Ag_2(THF)_2[Au(C_6F_5)_2]_2\}_n$ (**3**) also luminesce in the solid state at room temperature (Figures 3 and 7) and at 77 K.

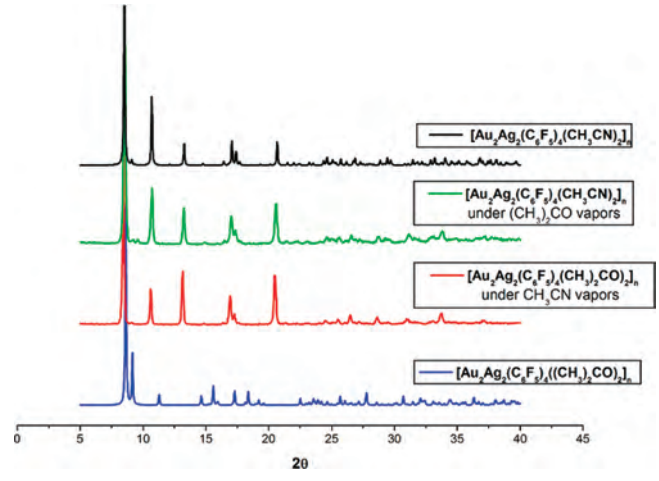

Figure 6. XPD patterns for VOC materials obtained by treatment of **2** (blue) with vapors of acetonitrile (red) or treatment of **4** (black) with vapors of acetone (red).

Scheme 1. Vapochromic Behavior of **1**−**4**

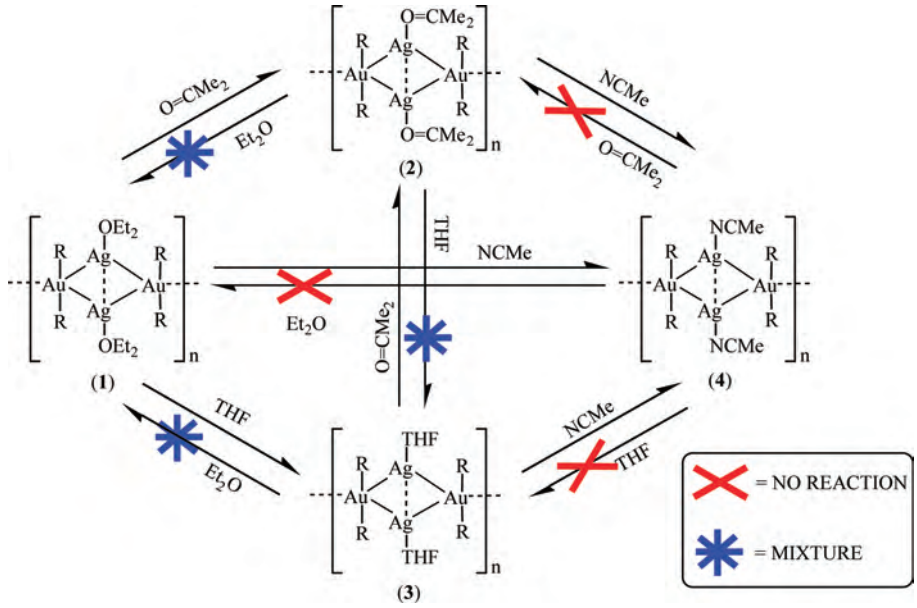

The excitation maxima (poorly defined) located at 468 nm (**1**) and 509 nm (**3**) lead to emission maxima at 585 nm (**1**) and 544 nm (**3**) at room temperature and at 605 nm (**1**) and 567 nm (**3**) at 77 K.

The lifetime measurements of the solid-state samples at room temperature [$\tau_1 = 431$ ns, $\tau_2 = 155$ ns, ($\chi^2 = 1.4$)] for **1**, together with the small Stokes' shift, suggest that the emission origin is associated with a spin-allowed fluorescent transition. However, the strong spin−orbit coupling of the heavy atoms in these complexes makes it difficult to reach a conclusive assignment. In the case of **3**, the lifetime is less precise because the solid undergoes a visible color change during the acquisition period, probably due to the loss of THF molecules. Also in this case, a biexponential decay is observed with a lifetime in the nanosecond time scale ($\tau_1 =$ 621 ns, $\tau_2 = 57$ ns), but the low-quality data fit ($\chi^2 = 23$) indicates that this assumption must be interpreted with caution.

The behavior in acetone solutions for both **1** and **3** is different from that reported for **2** and **4**.[16] In the later complexes, degassed acetone solutions (ca. 5×10^{-4} M) of the complexes became colorless and nonluminescent and evaporation of the solvent regenerates the initial color of the complexes and their optical properties, even after several solution/evaporation cycles. However, **1** and **3** became colorless when dissolved in acetone, but evaporation of the solvent does not regenerate the original complexes, and, instead, **2** is formed, in accord with the data and Scheme 1.

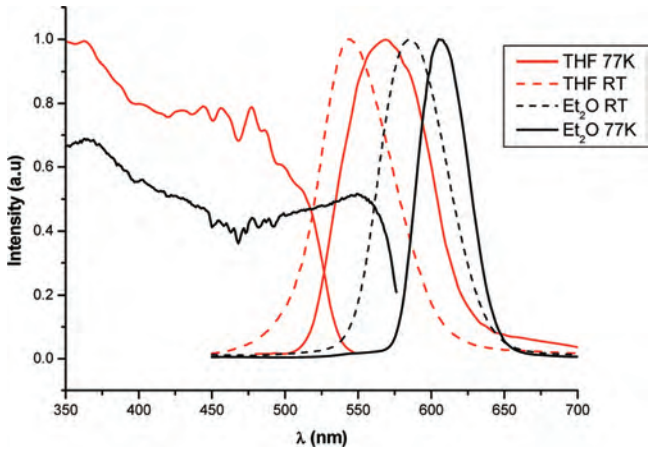

Figure 7. Excitation and emission spectra for **1** (black) and **3** (red) in the solid state at room temperature (dashed line) and at 77 K (line).

Interesting results are also obtained when the emission spectra of **1** and **3** are measured in glass media (EtOH/MeOH, v/v 1:4) at 77 K or in solution of the same mixture of alcohols at room temperature because both display emission maxima at similar wavelengths at both temperatures. Thus, in glass at 77 K both emit at 505 and 560 nm upon excitation at 450 nm. The fact that both display the same wavelength in the excitation and emission spectra suggests that the ground and excited states in both complexes are the same in the glass media. It is likely that in both cases the ligands, Et_2O and THF, are replaced by the stronger donors ethanol and methanol, giving rise to new oligomeric species. Thus, for instance, when **1** is dissolved in EtOH and frozen to 77 K, emissions at 513 and 546 nm appear. If the solvent used is MeOH, a single band at 538 nm is observed (Figure 8). However, the simultaneous presence of oligomers of different molecular weight in solution with different emission profiles cannot be excluded.

By contrast, solutions of **1** and **3** at room temperature display high-energy emission maxima (395 nm). It is likely that this is an emission from a localized excited-state on the pentafluorophenyl groups.[16] The loss of the low energy emissions arises from the rupture of the gold−gold interactions in the polymer as mediated by the donor solvents. In fact, **2** shows an emission at a similar wavelength to that previously reported,[16] and it was assigned to the same groups based on TD-DFT calculations. Nevertheless, MMCT transitions cannot be completely excluded, and the established

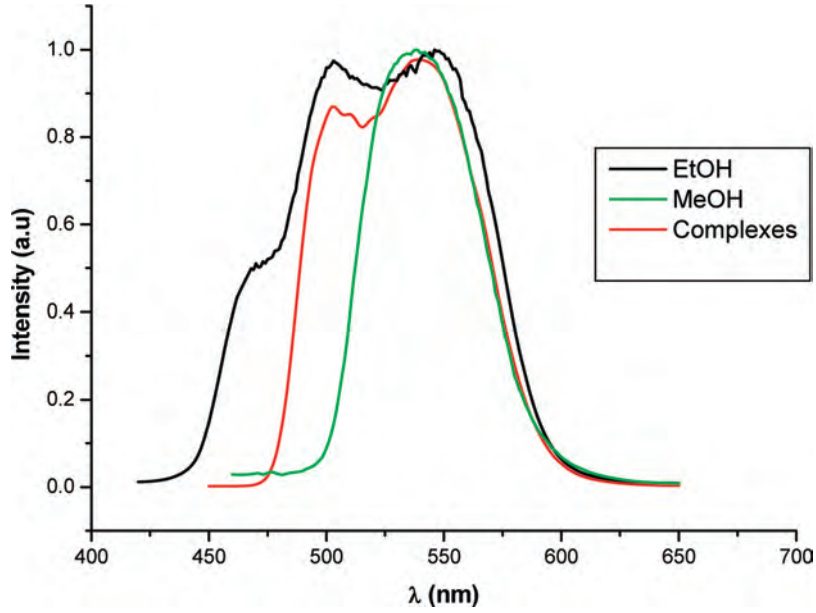

Figure 8. Emission spectra for **1** and **3** in glass media (EtOH/MeOH, v/v 1:4) (red), EtOH (black) and MeOH (green) at 77 K.

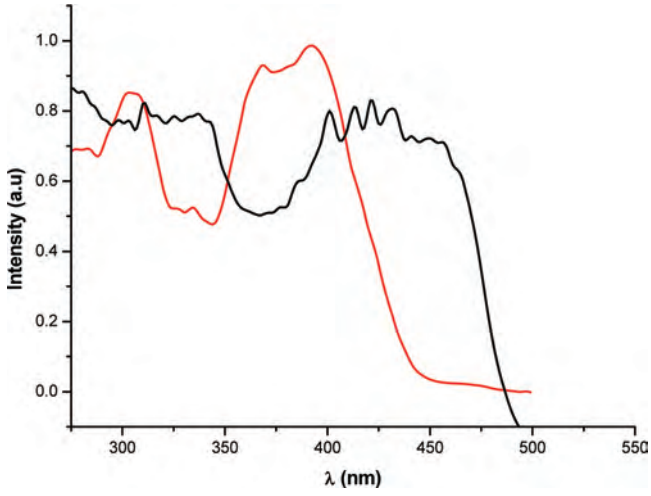

Figure 9. UV−vis absorption spectrum of **1** or **3** in glass media (EtOH/MeOH, v/v 1:4) at 77 K (black) and excitation spectrum of **1** or **3** in glass media (EtOH/MeOH, v/v 1:4) at 77 K (red).

crossover of σ and π states in the pentafluorophenyl units[21] clearly complicates a complete photophysical interpretation of the results at this time.

These excitation spectra results agree with the data obtained from the UV−vis spectra for **1** and **3** measured at room temperature in EtOH/MeOH, v/v 1:4 (5×10^{-4} M). Both show almost an identical profile with high energy bands at 242 nm ($\epsilon = 6.7 \times 10^3$) and 273 nm ($\epsilon = 6.3 \times 10^3$) for **1** and 238 nm ($\epsilon = 6.3 \times 10^3$) and 274 nm ($\epsilon = 6.1 \times 10^3$) for **3** ($\epsilon$ in units of liters per mole centimeters). On the basis of the high-energy absorptions and the similarity of the spectra for **1** and **3**, and the precursor complex $[Bu_4N][Au(C_6F_5)_2]$ (which displays broad bands at roughly similar energies and with similar intensities) we tentatively assign these adsorptions to allowed $\pi-\pi^*$ transitions in the pentafluorophenyl rings. A similar assignment has been described in other polymeric complexes built by acid/base stacking (acidic metal salts/basic bis(perhalophenyl)gold(I) anions),[4b,6,9] and for **2** and **4,** which display a similar behavior in donor solvents.[16] When the UV−vis measurements are carried out in a glass media at 77 K, in addition to the above-mentioned bands, intense absorptions at lower energies also appear. Thus, the spectra show complicated and almost identical profiles, with a low energy maximum at 430 nm. These absorption spectra roughly resemble the excitation spectra (low-energy maxima at 394 nm) (Figure 9), and thus it is likely that these low-energy absorptions give rise to the observed emissions that arise from excited states of singlet parentage. The corresponding absorption spectrum of the precursor $[Bu_4N][Au(C_6F_5)_2]$ salt in glass media does not display any absorption at a similar low energy.

Taking all the spectroscopic data presented here into account, a plausible origin of the emission spectra in these complexes is that the excited states responsible for the emissions are localized in the tetranuclear $[Ag_2L_2Au_2(C_6F_5)_2]$ cores, as previously suggested in DFT and TD-DFT calculations,[16,19] with energies which are influenced by the gold−gold or gold−silver interactions and by molecular aggregation.

Acknowledgment. The D.G.I.(MEC)/FEDER (CTQ2007-67273-C02-02) project and the Robert A. Welch Foundation of Houston, Texas, are acknowledged for financial support. R. C. Puelles thanks the Spanish MEC for a grant. This article is dedicated to the memory of Frank Albert Cotton, 1930−2007.

IC800452W

(20) Lifetime measurements were made by the pulse-modulation method. The success of the curve fits are given by χ^2 in the text. For both **1** and **3**, the best fit was done with two distinct lifetimes, both in the nanosecond range.

(21) Zgierski, M. Z.; Fujiwara, T.; Lim, E. C. *J. Chem. Phys.* **2005**, *122*, 144312/1–144312/6.